

Treatment of EXAFS data taken in the fluorescence mode in non-linear conditions

Gianluca Ciatto,^{a*} Francesco d'Acapito,^b Federico Boscherini^c and Settimio Mobilio^{d,e}

^aCNR, c/o ESRF, Gilda CRG, 6 Rue Jules Horowitz, F-38043 Grenoble, France, ^bINFM, c/o ESRF, Gilda CRG, 6 Rue Jules Horowitz, F-38043 Grenoble, France, ^cINFM and Department of Physics, University of Bologna, Viale Berti Pichat 6/2, 40127 Bologna, Italy, ^dDepartment of Physics, University of Roma Tre, Via della Vasca Navale 84, 00146 Roma, Italy, and ^eINFM, LNF, Via E. Fermi, I-00044 Frascati, Italy. E-mail: ciatto@esrf.fr

The aim of this work is to investigate the possibility of extracting correct structural parameters from fluorescence EXAFS data taken at high count rates with an energy-resolving detector. This situation is often encountered on third-generation synchrotron radiation sources which provide a high flux on the sample. Errors caused by pulse pile-up in the extraction of structural information have been quantified in a real experiment, and different approaches to the problem of data correction have been elaborated. The different approaches are discussed in a comparison of the ability of each kind of correction to recover the correct structural parameters. The result of our analysis is that it is possible to work in non-linear conditions and correct the data, if the response of the acquisition system is known. Reliable structural information can be obtained with data acquired up to a count rate equal to approximately 60% of the inverse of the dead time.

Keywords: detectors; dead time; pulse pile-up; EXAFS; non-linearity; fluorescence.

1. Introduction

Extended X-ray absorption fine-structure spectroscopy (EXAFS) is a powerful tool for investigating the local structure of materials. The aim of any EXAFS measurement is the determination, in the first few coordination shells, of local structural parameters around the excited atom: coordination numbers (N), interatomic distances (R) and Debye–Waller factors (σ^2). These parameters enter the expression for the EXAFS modulation of the absorption cross section, which, in the single-scattering and plane-wave approximation (Lee *et al.*, 1981), is

$$\chi(k) = \sum_i N_i A_i(k) \sin[2kR_i + \varphi_i(k)] \exp(-2k^2\sigma^2). \quad (1)$$

In this expression $A_i(k)$ and $\varphi_i(k)$ are the amplitude and phase shift of the backscattering function from atoms in the i th coordination shell [we have included many-body multiplicative terms in $A_i(k)$], k is the photoelectron wavevector and the sum is over all coordination shells.

When fluorescence detection is employed (Jaklevich *et al.*, 1977) the technique is able to probe the structure of atoms present in rather high dilutions or in thin films. The physical origin of this is that fluorescence detection isolates the signal of the excited atom from the total absorption of the matrix. Fluorescence detection is popular on EXAFS beamlines worldwide and has developed into a flexible experimental tool.

Solid-state energy-resolving detectors (Knoll, 1989) are often used in fluorescence EXAFS measurements. They allow, within the moderate energy resolution they possess (typically ~ 200 eV at

5.9 keV), the selection of the desired fluorescence line rejecting scattered photons and fluorescence lines coming from other absorbers. The limitation of this kind of detector is the relatively high dead time of the electronics used, needing several microseconds in order to sample the voltage signal with a sufficiently low statistical noise, thus causing pulse pile-up.

The aim of this work is to investigate the possibility of obtaining correct structural information when performing fluorescence EXAFS measurements with a high input count rate; the particular case of a high-purity Ge detector coupled to digital electronics is addressed. There are at least two reasons why this study is relevant, both relating to the high-brilliance beams provided by state-of-the-art beamlines on third-generation synchrotron radiation sources. If the spectrum of photons scattered from the sample is dominated by the fluorescence line of interest, recording data at high-count rate allows the reduction of the total acquisition time per spectrum. Fluorescence yield detection has been successfully extended even to the case of concentrated samples providing that self-absorption is either minimized by an appropriate low-exit angle geometry or accounted for by using appropriate corrections (Hayes & Boyce, 1983; Tröger *et al.*, 1992; Eisebitt *et al.*, 1993; Pfalzer *et al.*, 1999). If, on the other hand, the fluorescence line of interest represents only a minor fraction of photons scattered from the sample, it might be inevitable to perform the experiment with a high number of total photons impinging on the detector in order to have a sufficient count rate in the region of interest.

It has been generally recognized that when high count rates are used dead-time effects can be important, the most well known effect being an artificial decrease of the amplitude of the EXAFS signal. It is possible to recover such errors, by using suitable corrections, as already observed by different groups (Cramer *et al.*, 1988; Dent *et al.*, 1995; Farrow *et al.*, 1998; Nomura, 1998). Even if the problem is, in general, well known, a quantitative and systematic study of the effect of dead-time losses on the structural parameters extracted from EXAFS data, and of the reliability of dead-time corrections in recovering the correct structural information, is at present missing in the literature.

In this paper three different approaches to the data-correction problem are presented. For each approach we estimate the maximum count rate up to which the particular kind of correction can be used, by considering the deviation of the evaluated structural parameters with respect to the known values in a model sample.

In this work we assume that the fluorescence intensity is directly proportional to the absorption coefficient of the excited atom, *i.e.* that self-absorption effects are negligible or can be subsequently corrected.

2. Data-correction methods

There are two models of dead-time behaviour for pulse-counting systems: the paralyzable and the non-paralyzable response (Knoll, 1989). It is recognized that solid-state detectors used for X-ray spectroscopy and the associated electronics have a paralyzable response function, so we will focus on this model here. For a paralyzable response function a dead time τ is assumed to follow each true event that occurs during the live period of the detector. True events that occur during the dead period, although not recorded as counts, extend the dead time by another period τ following the last lost event.

If we call n the *true* count rate (*i.e.* the real rate of photons impinging on the detector), m the *apparent* count rate (*i.e.* the rate measured by the pulse-counting electronics) and τ the system dead

time, statistical considerations (Knoll, 1989) lead to the following relation for the system throughput,

$$m = n \exp(-n\tau). \quad (2)$$

This relation is, strictly speaking, valid for the total, *i.e.* the energy-integrated, count rates. In discussing possible data-correction strategies we assume that the system dead time τ has been measured (in our experiment we determined it in a way which will be explained in §4) and that it is possible to measure, for every energy point E in the EXAFS scan, the ratio between the true energy-integrated count rate (using an amplifier channel with negligible dead time) and the corresponding apparent energy-integrated count rate (measured with an amplifier dead time τ). We will call these two count rates $n_T(E)$ and $m_T(E)$ and distinguish them from $n_F(E)$ and $m_F(E)$ which refer to the count rates in the region of interest of the selected fluorescence line. The amplifier channel with low dead time will be referred to as the ‘fast’ channel and the amplifier channel with non-negligible dead time as the ‘slow’ channel. The ratio between $n_T(E)$ and $m_T(E)$ is automatically recorded in our acquisition output file, together with $m_F(E)$, for each detector element.

We will discuss three methods to correct the data taken at high count rates.

2.1. Numerical inversion (method I)

The system throughput relation, equation (2), can be numerically inverted to extract the *true* count rate $n(E)$ from $m(E)$, providing that the dead time τ is known. As the raw signal to be treated is given by the fluorescence count rate $m_F(E)$ whereas equation (2) is rigorously valid for total count rates $m_T(E)$, first we have to modify $m_F(E)$ in order to obtain a variable [that we will call simply $m(E)$] which mimics the magnitude of $m_T(E)$. This is necessary in order to perform the inversion on the correct point of the non-linearity curve and can be done by multiplying $m_F(E)$ by a constant (namely to consider the presence of the K_β line when measuring the K_α) and/or by adding a constant to account for the scattered radiation (elastic and inelastic) plus possible fluorescence from lighter elements. A method to carry out the conversion of $m_F(E)$ into $m(E)$ is described below.

Then the numerical inversion is undertaken on the variable $m(E)$ by means of a Fortran code developed by the authors.† The inversion routine first assigns, for each energy point, the value $m(E)$ to the variable $n(E)$; then it calculates a new value of $m(E)$ by using equation (2). If the calculated $m(E)$ [that we will call $m_c(E)$] is smaller than the measured $m(E)$ and if the absolute value of the difference between the two is greater than $m(E)/\varepsilon_1$, where ε_1 is a fixed parameter, $n(E)$ is incremented by $n(E)/\varepsilon_2$ and another $m_c(E)$ is calculated through the equation starting from the new $n(E)$. The process is iterated until $m_c(E)$ approaches the measured $m(E)$ within a tolerance parameter $m(E)/\varepsilon_1$, the value of $n(E)$ which generates the last value of $m_c(E)$ is kept as the definitive true value.

ε_1 and ε_2 are, respectively, the tolerance and the step parameter of the iteration which yields, at the end, the ‘true’ count rate $n(E)$ for each energy point; they determine the systematic error on the extracted value of $n(E)$ and they can be easily assigned different values according to users’ requests; for our purpose the values of $\varepsilon_1 = 2000$ and $\varepsilon_2 = 500$ were found to give excellent results. The choice of these values depends on the signal count rate; the systematic error is in fact, at most, equal to the step $n(E)/\varepsilon_2$ and must be kept below the statistical one. If $n(E)$ follows Poisson’s statistics the error on it is given by its square root, so in our case the systematic error is surely

† *Invert3b* (Fortran77 program). The code is available, on request, from the contact author: ciatto@esrf.fr.

under the statistics level when $n(E)/500 \leq n(E)^{1/2}$, *i.e.* when $n(E) \leq 250000$ counts s^{-1} .

In our experiment the energy-integrated count rate on the fast channel is at the most 132000 counts s^{-1} ; $n(E)$ is, of course, even smaller and always ≤ 90000 above the edge for each channel and for each spectrum; for the last point we claim to be able to correct, $n(E)$ is ≤ 70000 for each channel above the edge. It follows that the correction procedure is always applicable, with the chosen values for the parameters. Output obtained by increasing both the parameters by a factor of ten was checked to be virtually identical. It is clear that the code could be easily modified to cope with higher count rates, paying a price in terms of computation time.

The program checks if the input value of $m(E)$ is compatible with the selected peaking time of the system; also it ends the iteration when $m_c(E)$ starts decreasing as the number of iteration increases, keeping the last positive-derivative value, in case numerical approximations lead to a point above the peak of the non-linearity (NL) function.

2.2. Correcting by the measured system lifetime (method II)

Starting from equation (2), the system throughput $\exp(-n\tau)$ can be experimentally determined by measuring at each energy point the energy-integrated count rates $n_T(E)$ and $m_T(E)$ exploiting the two amplifier channels,

$$\exp(-n\tau) = m_T(E)/n_T(E) = 1/C(E).$$

If we assume that the fast-channel dead time in measuring the energy-integrated count rate is negligible and that the correction factor $C(E)$, obtained from the energy-integrated count rates, is applicable to any subset of photons (*i.e.* dead-time losses are energy independent), then the true count rate in the region of interest is obtained at each energy as

$$n_F(E) = m_F(E) C(E). \quad (3)$$

2.3. Linearization (method III)

Since the EXAFS effect is a normalized weak modulation of the absorption coefficient $\mu(k)$ it is reasonable to propose a linearization of the system throughput function, equation (2). The EXAFS signal $\chi(k)$ is given by

$$\chi(k) = \frac{\mu(k) - \mu_0(k)}{\mu_0(k)} \simeq \frac{n(k) - J}{J}, \quad (4)$$

which implies

$$n(k) = J[\chi(k) + 1].$$

Here, $\mu_0(k)$ is the atomic absorption coefficient, $n(k)$ is the true fluorescence count rate in the region of interest and J is the true fluorescence ‘jump’, *i.e.* the discontinuity in the absorption coefficient at the absorption edge. We have approximated the atomic background function $\mu_0(k)$ with the constant edge jump, which is reasonable for samples with a well defined and ordered structure as in our case (in the inset of Fig. 1 we report a raw fluorescence spectrum).

In a real experiment, because of pulse pile-up, we measure neither $n(k)$ nor J but a function R of these quantities, which is the same as equation (2),

$$R(y) = y \exp(-\tau y).$$

In making this choice we perform a significant approximation because we extend equation (2), which is rigorously valid for the energy-integrated counts, to a subset of photons corresponding to the

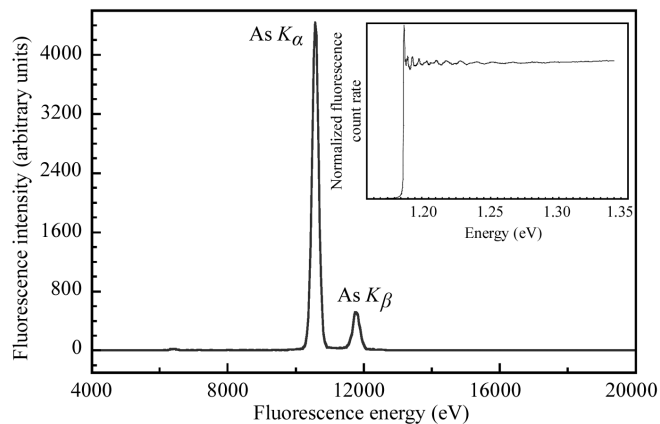


Figure 1 Spectrum of photons emitted from the InAsP sample, dominated by As K_α and As K_β fluorescence lines. The inset shows a typical raw absorption spectrum.

fluorescence line of interest. The pulse-counting electronics actually respond to the total count rate, so by using this approximation we are not working on the correct point of the NL curve, but on a less critical one at lower count rates.

On the other hand, as long as the fast total count rate does not become too close to the NL curve maximum, it is reasonable to perform corrections both on the different EXAFS scan points $m_F(E)$ and on the measured jump in the same point of the NL curve. Owing to the definition of EXAFS in equation (4), the two terms compensate and variations in the amplitude of $\chi(k)$ are not too severe moving through the NL curve, keeping sufficiently far away from the maximum (see §5).

Therefore, the measured EXAFS signal, $\chi_m(k)$, is

$$\chi_m(k) = \frac{R[n(k)] - R(J)}{R(J)},$$

which, with the approximation $\tau J \ll 1$ (moderate pile-up), becomes

$$\chi_m(k) = \frac{n(k)[1 - \tau n(k)] - J(1 - \tau J)}{J(1 - \tau J)} = \chi(k) \left[1 - \frac{\tau n(k)}{1 - \tau J} \right].$$

Straightforward manipulations lead to

$$\begin{aligned} \chi_m(k) &= \chi(k)[1 - B(k)], \\ B(k) &= \frac{\tau J}{1 - \tau J} [1 + \chi(k)] \simeq \tau J, \\ \chi(k) &\simeq \chi_m(k)[1/(1 - \tau J)]. \end{aligned} \quad (5)$$

According to this expression the dead-time correction on $\chi_m(k)$ is an overall amplitude factor and depends only on the product between the dead time and the true value of the fluorescence jump; the latter can be obtained by using one of the two previous methods.

The appearance of only an overall amplitude reduction implies that the only effect predicted on the structural parameters is a reduction of the estimated coordination numbers, without any effect on interatomic distances or Debye–Waller factors. Equation (5) gives us the simplest way to correct data for dead-time losses: we can perform a conventional quantitative analysis starting from the extracted $\chi_m(k)$ and correct *a posteriori* the obtained coordination numbers by the term $(1 - \tau J)^{-1}$.

3. Experimental

In order to check the applicability of the correction methods presented above we have performed test experiments at the GILDA

CRG beamline of the European Synchrotron Radiation Facility in Grenoble, France. The monochromator was equipped with a pair of Si(311) crystals and run in the so-called dynamical focusing mode (Pascarelli *et al.*, 1996).

The sample analyzed was an InAs_{0.36}P_{0.64} polycrystalline alloy grown on Al substrate (Pascarelli *et al.*, 1997). In this context the advantage of using this sample is the well defined local structure around As (four In atoms at equal distance in the first coordination shell). Moreover, the thickness of the epilayer was 30 μm and this guaranteed intense As K_α and K_β fluorescence lines; in fact, the spectrum of photons emitted from the sample is dominated by these fluorescence lines with negligible contribution from elastic or Compton scattering as shown in Fig. 1. The detector is placed at 90° to the impinging beam in the horizontal plane and the sample surface forms an angle of 45° with the incident and fluorescence beams.

Since the filling mode of the storage ring was uniform, the dead time of our acquisition system was by far bigger than the time interval between electron bunches. Furthermore, at any used count rate there was very much less than one detectable event per bunch. In this condition the arrival of events on the detector can be considered random in time and the experiment was not sensitive to the beam time structure, which allowed us to use the standard equation (2) as an expression of the system throughput. Different formulations need to be employed in the case of few bunches or in single-bunch mode when the time separation between two bunches (corresponding to the circuit of the ring in the latter case) is comparable with the electronics dead time (Bateman, 2000).

The detector used was a 13-element high-purity germanium model (EG&G ORTEC, model IGLET-11150X7-S), the preamplifier model was 239R, the active diameter was 11.3 mm, and the average energy resolution (FWHM) for the 13 elements with an Fe⁵⁵ source and 1000 counts s⁻¹ was about 290 eV with a 1 μs peaking time constant and about 265 eV with a 4 μs peaking time constant. The detector elements were arranged symmetrically on two circles centered on the central element. The pulse-processing electronics was a digital X-ray processor (DXP) manufactured by XIA (model 4C/4T, revision C†; DXP Board revision C, DSP code revision 1.05, FIPPI Firmware revision C); this electronics has trapezoidal fast and a slow amplifier channels which run at the same time, thus allowing data correction according to method II outlined above. Each detector element is coupled to an independent pulse-processing electronics channel. The fast amplifier channel has a dead time equal to 0.8 μs , and can be used to count almost all the photons that arrive on the detector. The peaking time for the slow amplifier channel was set for the series of measurements reported here to 4 μs , which corresponds to a nominal dead time of 8.2 μs ; this rather high value was chosen to highlight the system non-linearity.

4. Results

As a first step, the system throughput was determined at fixed incoming photon energy (12500 eV) by measuring the fluorescence count rate in the slow amplifier channel as a function of the energy-integrated count rate recorded in the fast channel. This was achieved by varying the intensity of the beam impinging on the sample using filters, different relative alignment of the monochromator crystals and different sample–detector distances. The system throughput was fitted with equation (6) and the result is shown in Fig. 2. The fit gave $\tau = 9.1 \mu\text{s}$, in reasonable agreement with the expected value.

† For a description see <http://www.xia.com>.

$$m_F = an_T \exp(-n_T \tau). \quad (6)$$

Equation (6) is similar to equation (2), where the constant a was introduced to take into account that the fluorescence count rate measured on the slow channel substitutes for the total count rate in the formulation; the best fit gives a value of 0.87 for this constant. The inverse of a provides us with a factor to convert the K_α fluorescence count rate into energy-integrated count rate and it was exploited while correcting by method I, as described above. Since the total count rate, excluding K_α counts, is in this case essentially given by the K_β line and the intensity ratio between the two fluorescence lines being energy independent, the value determined for a at about 600 eV above the As edge is valid all over the EXAFS scan, otherwise knowledge of the entire function $m_T(E)$ might be necessary. The function in equation (6) increases monotonically until $n_T = 1/\tau$, where it has a maximum, after which it decreases and goes to zero as n_T increases further; the true count rate corresponding to the maximum of the NL curve ($n_T = 1/\tau$) can be considered a characteristic frequency of the acquisition system.

EXAFS spectra at the arsenic K edge were collected at various fast energy-integrated count rates (6–132 Kcounts s^{-1} , i.e. 5–120% of the characteristic frequency) taking care to adjust the integration times in order to keep the number of counts per energy point as constant as possible. The count rates, here and in the following, refer to each detector element. The spectra will be labelled with the fast energy-integrated count rates measured on the central detector element. For

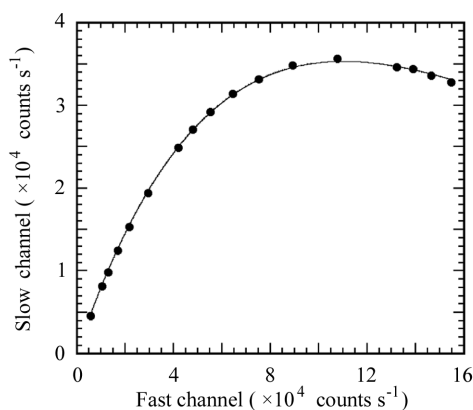


Figure 2
Response of the slow channel of the counting electronics as a function of the total count rate, measured by the fast channel. Dots: experiment; continuous line: fit with equation (6).

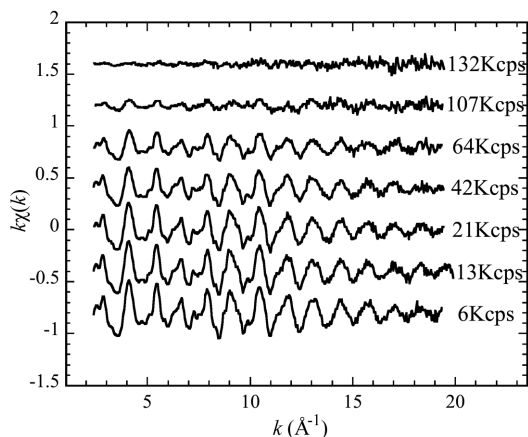


Figure 3
Uncorrected EXAFS data obtained at different total count rates.

correction methods I and II the signal from each detector element was first corrected, in order to take into account the different count rates, and then the average of these spectra was calculated and quantitatively analysed as described below. For method III an average spectrum was calculated, then analysed and the corrected coordination number subsequently calculated according to equation (5).

EXAFS spectra (in the energy range 11650–13400 eV) were recorded by monitoring the intensity of the K_α fluorescence line with the slow amplifier channel; at the same time, the ratio $C(E)$ (equation 3) between the energy-integrated count rates measured with the fast and the slow channels was recorded. This procedure was carried out for each of the 13 detector elements. Quantitative data analysis was performed with the experimental standard method using the package by Michalowicz (1997). EXAFS oscillations were extracted by fitting the pre-edge background using a linear function and by using a fifth-order polynomial to model the atomic background. Fig. 3 reports the uncorrected background-subtracted EXAFS spectra: the progressive distortion of the signal with increasing count rate is apparent; when the total count rate reaches 107 Kcounts s^{-1} (97% of $1/\tau$) the EXAFS oscillations are almost completely smoothed out.

The data were corrected by the methods I and II and the corresponding EXAFS spectra are shown in Figs. 4 and 5. For the uncorrected spectra and for each data-correction method the spectrum taken at the lowest count rate (6 Kcounts s^{-1}) was used as a reference

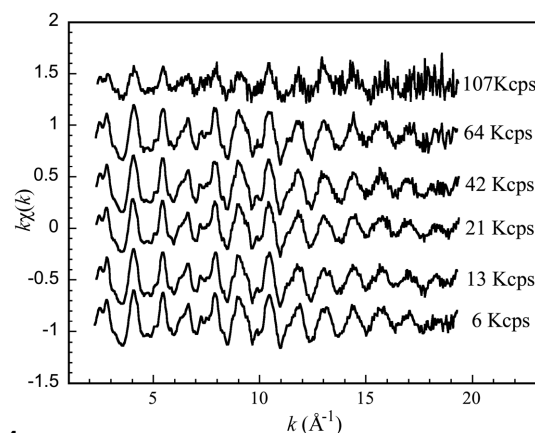


Figure 4
EXAFS data corrected by numerical inversion of the non-linear system response (method I).

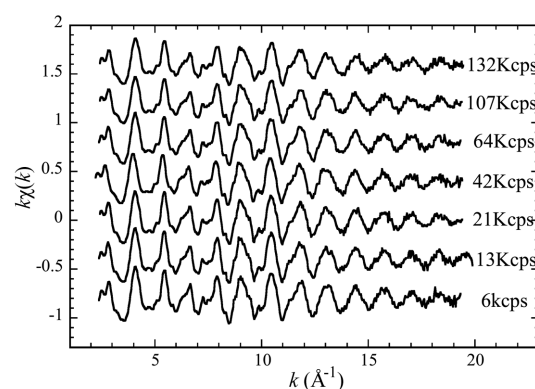


Figure 5
EXAFS data corrected by multiplying the fluorescence rate by the ratio of the total count recorded in the fast amplifier channel to those in the slow amplifier channel (method II).

Table 1

Structural parameters obtained from the uncorrected spectra and from those corrected using methods I and II.

N: coordination number; *R*: interatomic distance; σ^2 : Debye–Waller factor. Error bars are calculated from a χ^2 analysis at the 90% confidence level.

Total count rate (Kcounts s ⁻¹)	<i>N</i> (atoms)	<i>R</i> (Å)	σ^2 (10 ⁻³ Å ²)
Uncorrected data			
13	3.75 ± 0.54	2.584 ± 0.004	2.6 ± 0.6
21	3.42 ± 0.45	2.583 ± 0.004	2.6 ± 0.6
42	2.76 ± 0.32	2.584 ± 0.003	2.5 ± 0.5
64	2.04 ± 0.36	2.580 ± 0.009	2.5 ± 0.1
107	0.70 ± 0.35	2.582 ± 0.029	2.5 ± 2.0
132	0.30 ± 0.60	2.586 ± 0.142	4.9 ± 9.2
Method I			
13	3.99 ± 0.46	2.584 ± 0.006	2.5 ± 0.5
21	4.06 ± 0.57	2.582 ± 0.004	2.5 ± 0.6
42	4.04 ± 0.51	2.583 ± 0.004	2.4 ± 0.7
64	3.84 ± 0.59	2.581 ± 0.005	2.5 ± 0.5
107	1.92 ± 0.79	2.580 ± 0.012	2.0 ± 1.6
Method II			
13	4.00 ± 0.32	2.585 ± 0.004	2.6 ± 0.4
21	3.93 ± 0.28	2.583 ± 0.004	2.6 ± 0.3
42	3.84 ± 0.20	2.585 ± 0.003	2.6 ± 0.2
64	3.71 ± 0.49	2.583 ± 0.004	2.5 ± 0.6
107	3.50 ± 0.20	2.582 ± 0.002	2.6 ± 0.3
132	3.47 ± 0.23	2.581 ± 0.004	2.8 ± 0.3

to extract experimental amplitudes and phases; the first shell structural parameters were determined using a non-linear fitting routine in which these parameters, along with an energy origin shift, were varied until a best fit was found. The following structural values were taken as a reference, based on the known structure of the sample: *N* = 4, *R* = 2.582 Å, $\sigma^2 = 2.5 \times 10^{-3}$ Å². The values obtained from the fitting procedure are reported in Table 1 as a function of the energy-integrated count rate measured in the fast channel. We point out that the strongest effect of the distortions induced by the high count rates is on the coordination numbers while the other structural parameters are practically unaffected within the error bars. For method III, the correction to the coordination numbers was applied *a posteriori* to the values obtained from the analysis of the uncorrected data. The As coordination numbers obtained by using the three methods as a function of the total counting rate are shown in Fig. 6.

5. Discussion

The progressive distortion of the EXAFS signal with increasing count rate (Fig. 3) makes it impossible to evaluate correctly the As coordination number if corrections are not applied. With a true total count rate of 42 Kcounts s⁻¹ (38% of 1/ τ) the coordination number obtained from the uncorrected data corresponds to 70% of the true value (see Fig. 6), a deviation which is well above the statistical error bar and is thus unacceptable.

Correction method I permits the evaluation of reasonable As coordination numbers (96% of the true value) up to 64 Kcounts s⁻¹ (58% of 1/ τ), the as-determined values are identical within the statistical error bar. Above 60% of the characteristic frequency method I is unreliable and evaluated coordination numbers exhibit very large deviation from the known values. Here, m_T begins to saturate and oscillations in m_F become comparable with statistical noise; the numerical inversion, performed in a region in which the NL curve has a low slope, expands both the signal and the noise providing a very noisy $n_F(E)$ from which it is impossible to recover correct structural information. Finally, method I cannot be applied to the last point at 132 Kcounts s⁻¹ in Fig. 6, beyond the NL maximum, because

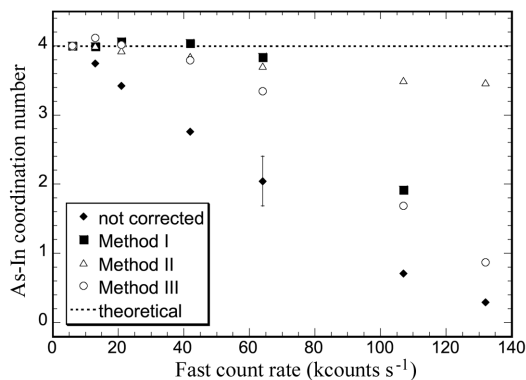


Figure 6

Arsenic coordination numbers evaluated from uncorrected data and from data corrected using methods I, II and III as a function of the total count rates. For clarity, only one typical error bar is reported.

it cannot treat multi-values functions since the numerical iteration stops as the non-linearity curve peak is reached. It is worth remarking that the possibility of working at 60% of 1/ τ might appear surprising because it is rarely exploited by experimentalists, most probably due to a lack of quantitative information on the recovering power of dead-time corrections: if a peaking time of 1 μ s was employed (this is the more common choice for most experiments), this correction method is expected to be adequate up to 260 Kcounts s⁻¹.

Correction with method II appears to be a little worse than with method I until 60% of 1/ τ (93% of the true values). On the other hand it becomes more powerful than method I at very high count rates, near and beyond the characteristic frequency, where it is able to recover a signal of good quality (Fig. 5) and quite reasonable values for the coordination numbers (87% of the true value at 132 Kcounts s⁻¹). It must be noted, however, that this remarkable effect is due to the presence of an EXAFS signal in the correction factor *C(E)* itself. In fact, since *C(E)* is the ratio between the total counts recorded by the fast channel and those recorded by the slow one, at very high count rates the denominator is practically constant because of pile-up while the numerator continues to oscillate. The corrected spectrum is the product of the apparent count rate of the selected fluorescence signal, which is virtually constant, and the oscillating correction factor. The correction works very well in this case because the spectrum of photons reaching the detector is dominated by the As *K α* fluorescence line; if the selected line represented only a small fraction of the total counts the oscillations present in *C(E)* would be much weaker compared with the baseline, and the resulting $n_F(E)$ near NL maximum would be as noisy as for method I or even worse in the case of high dilution for the element of interest. Actually, when applying method II at very high count rates in the present case, we are not exploiting the energy resolution of the detector. The peculiarity of method II is that it exploits the energy resolution of the acquisition when it is possible, otherwise it automatically uses the fast channel.

Correction with method III provides a very simple way of correcting data, applying an overall factor directly on coordination numbers extracted from uncorrected data. On the other hand, considering the strong approximation involved in this procedure, the lower recovering power of this kind of approach should not be surprising. As shown in Fig. 6, method III allows the evaluation of reliable coordination numbers (95% of the true value) up to 42 Kcounts s⁻¹ (38% of 1/ τ). At a count rate of 64 Kcounts s⁻¹ (58% of 1/ τ), however, the coordination numbers obtained using method III are \sim 80% of the correct value, a deviation which is unacceptably

large compared with the statistical error bar. Corrections applied to data taken at even higher count rates (107 and 132 Kcounts s^{-1}) dramatically fail: this method relies on the assumption that $J\tau \ll 1$, which here is clearly not valid. By choosing this simplification we 'lose' the range 40–60% of $1/\tau$ because, as long as we remount the NL curve and the local derivative becomes flatter and flatter, the approximation for which it is possible to correct all the energy points of the EXAFS scan on the same point of the NL curve does not work any more and the correction on the jump does not normalize the correction on m_F .

Even if method III is less powerful than the others it permits the evaluation of reliable structural information up to 160 Kcounts s^{-1} if a peaking time of 1 μs is chosen, well above the fast count rates commonly used in fluorescence EXAFS experiments. On the other hand, it does not require the point-to-point knowledge of $n_T(E)$ and $m_T(E)$, nor the numerical inversion of $m_F(E)$: knowledge of the two parameters in equation (6) is in fact sufficient and they can be determined by measuring a few points and performing a simple fit, as we did in this paper.

6. Conclusions

We have performed a quantitative study of the effects of dead-time losses on the evaluation of structural parameters from EXAFS data taken in the fluorescence mode at high count rates. If no corrections are performed, pulse pile-up results in a severe decrease of the estimated coordination numbers, while interatomic distances and Debye–Waller factors are not affected. Different kinds of approaches to the correction problem have been tested and compared. A method based on the numerical inversion of the throughput of the pulse-counting electronics allows the recovery of the correct value of the coordination number within a 4% deviation up to count rates corresponding to $\sim 60\%$ of the inverse dead time. Beyond 60%, this

method fails and another one, which exploits the measured system lifetime, has to be considered to be the most efficient.

The authors would like to thank P. L. Solari for valuable help during the measurements, and S. Colonna, C. Meneghini and V. Sciarra for useful discussions. The experiment was performed at GILDA CRG, ESRF, by using IHR (In-House Research) beam time.

References

- Bateman, J. E. (2000). *J. Synchrotron Rad.* **7**, 307–312.
- Cramer, S. P., Tench, O., Yocum, M. & George, G. N. (1988). *Nucl. Instrum Methods Phys. Res. A*, **266**, 586–591.
- Dent, A. J., Derbyshire, G. E., Derst, G. & Farrow, R. C. (1995). *Rev. Sci. Instrum.* **66**, 2306.
- Eisebitt, S., Böske, T., Rubensson, J.-E. & Eberhardt, W. (1993). *Phys. Rev. B*, **47**, 14103–14109.
- Farrow, R. C., Headspith, J., Dent, A. J., Dobson, B. R., Bilsborrow, R. L., Ramsdale, C. A., Stephenson, P. C., Brierley, S., Derbyshire, G. E., Sangsingkeow, P. & Buxton, K. (1998). *J. Synchrotron Rad.* **5**, 845–847.
- Hayes, T. M. & Boyce, J. B. (1983). *Solid State Physics*, Vol. 37, edited by H. Ehrenreich, F. Seitz and D. Turnbull, pp. 256–351. New York: Academic Press.
- Jaklevich, J., Kirby, J. A., Klein, M. P., Robertson, A. S., Brown, G. S. & Eisenberger, P. (1977). *Solid State Commun.* **23**, 679–682.
- Knoll, G. F. (1989). *Radiation Detection and Measurement*, ch. 4. New York: Wiley.
- Lee, P. A., Citrin, P. H., Eisenberger, P. & Kincaid, B. M. (1981). *Rev. Mod. Phys.* **53**, 769–806.
- Michalowicz, A. (1997). *J. Phys. IV*, **7**(C2), 235–236.
- Nomura, M. (1998). *J. Synchrotron Rad.* **5**, 851–853.
- Pascarelli, S., Boscherini, F., d'Acapito, F., Hrdy, J., Meneghini, C. & Mobilio, S. (1996). *J. Synchrotron Rad.* **3**, 147–155.
- Pascarelli, S., Boscherini, F., Lambertini, C. & Mobilio, S. (1997). *Phys. Rev. B*, **56**, 1936–1947.
- Pfalzer, P., Urbach, J.-P., Klemm, M., Horn, S., den Boer, M. L., Frenkel, A. I. & Kirkland, J. P. (1999). *Phys. Rev. B*, **60**, 9335–9339.
- Tröger, L., Arvanitis, D., Baberschke, K., Michaelis, H., Grimm, U. & Zschech, E. (1992). *Phys. Rev. B*, **46**, 3283–3289.